Reflection Characteristics of a PML With a Shallow Corrugation

Marina E. Inchaussandague, Miriam L. Gigli, and Ricardo A. Depine

***Abstract*—The constitutive characteristics of anisotropic materials can be exploited to construct absorbers that provide reflectionless interfaces for waves at arbitrary angles of incidence. In this paper, we investigate how a weak corrugation affects the reflectivity of the anisotropic perfectly matched absorber developed by Sacks *et al.* for a flat interface. To do so, we develop a Rayleigh method to calculate the fields diffracted at the periodically corrugated boundary of an anisotropic absorber with constant constitutive tensors, which correspond to a planar (Cartesian) perfectly matched layer. We present numerical results in the nondiffractive regime (where only a specularly reflected wave can propagate) for sinusoidal corrugations with different groove height-to-period ratios. Our results show that the reflectivity of the anisotropic absorber near normal incidence remains very low (less than 0.4% for a 10% modulation), whereas it changes dramatically near grazing incidences.**

***Index Terms*—Absorber, anisotropy, perfectly matched layer (PML), reflectivity, scattering.**

I. Introduction

THE perfectly matched layer (PML) approach is a powerful formulation to solve unbounded electromagnetic problems. Two types of PMLs are to be distinguished: the first, introduced by Berenger [1], [2], is based on a splitting of each Cartesian field component into two subcomponents and the second, given by Sacks *et al.* [3], is based on anisotropic material properties chosen in such a way that a plane interface between the anisotropic medium and free space is perfectly reflectionless for any angle of incidence, frequency, and polarization. Unlike Berenger's PML, the anisotropic perfectly matched absorber has the advantage of not requiring any modification of Maxwell's equations.

The original PML concept applied to only Cartesian coordinates planar interfaces. To extend its range of applicability, other reflectionless absorbers have been developed for nonplanar interfaces, such as, for example, two-dimensional (2-D) cylindrical, three-dimensional (3-D) cylindrical, and 3-D spherical interfaces [4]–[6]. For a general concave boundary, a conformal PML with constitutive tensors dependent on the local radii of curvature of the surface has been developed in [7]. However, the behavior of the conformal PML is strongly dependent of the local geometry of the termination since, for convex surfaces (negative local radius), the analysis is dynamically unstable [8]. Due to this limitation, the concept of a conformal PML cannot be applied to the study of boundaries, such as the rough interface considered here, which are neither concave nor convex. Since the extension of the Cartesian PML concept to rough boundaries could be useful for the analysis of devices combining stratification and corrugation, in this paper we investigate how a weak corrugation affects the reflectivity of the otherwise reflectionless anisotropic absorber with constant constitutive tensors. To do so, we develop a Rayleigh method to calculate the fields diffracted at the periodically corrugated boundary between free space and an anisotropic absorber. This method is based on the assumption that the electromagnetic fields in the region between the grooves can be written as plane-wave expansions [9]. Although not rigorous, Rayleigh methods have proven to give very good results for corrugated isotropic [10], [11], gyroelectromagnetic [12], and anisotropic [13], [14] gratings, even for groove height-to-period ratios greater than 0.14, the limit of validity of the hypothesis for perfect conductors with sinusoidal corrugation.

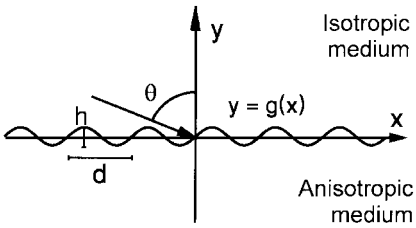

Fig. 1. View of the principal section of the grating.

II. Theory

We consider a periodically corrugated interface given by $y = g(x) = g(x + d)$ (d is the period), separating an isotropic medium from an anisotropic absorbing medium (Fig. 1). The z-axis is placed along the grooves and the y-axis, perpendicular to the mean surface of the grating, is directed toward the isotropic medium. Harmonic time dependence $\exp(-i\omega t)$ is assumed and omitted throughout the paper.

The isotropic region ($y > g(x)$) is characterized by the following constitutive relations:

$$\vec{D} = \epsilon_0 \epsilon \vec{E} \tag{1}$$

$$\vec{B} = \mu_0 \mu \vec{H} \tag{2}$$

Manuscript received July 6, 2002; revised November 13, 2002. This work was supported by the Consejo Nacional de Investigaciones Científicas y Técnicas under a grant and by the Agencia Nacional de Promoción Científica y Tecnológica under Grant ANPCYT-BID 802/OC-AR03-04457.

The authors are with the Grupo de Electromagnetismo Aplicado, Departamento de Física, Facultad de Ciencias Exactas y Naturales, Universitaria de Buenos Aires, Ciudad Universitaria, 1428 Buenos Aires, Argentina and also with the Consejo Nacional de Investigaciones Científicas y Técnicas, Rivadavia 1917, Buenos Aires, Argentina.

Digital Object Identifier 10.1109/TMTT.2003.812566

where $\epsilon_0\epsilon$ and $\mu_0\mu$ are the permittivity and permeability of the dielectric medium and ϵ_0 and μ_0 are, respectively, the permittivity and permeability of the vacuum.

The absorbing anisotropic side ($y < g(x)$) is characterized by

$$\vec{D} = \epsilon_0 \tilde{\epsilon} \cdot \vec{E} \tag{3}$$

$$\vec{B} = \mu_0 \tilde{\mu} \cdot \vec{H} \tag{4}$$

where $\tilde{\epsilon}$ is the dielectric tensor and $\tilde{\mu}$ is the permeability tensor of the material. Following Sacks *et al.* [3], we consider the case in which $\tilde{\epsilon}$ and $\tilde{\mu}$ are diagonal tensors given by

$$\tilde{\mu} = \mu\tilde{\Lambda} = \mu \begin{pmatrix} a & 0 & 0 \\ 0 & b & 0 \\ 0 & 0 & c \end{pmatrix} \tag{5}$$

$$\tilde{\epsilon} = \epsilon\tilde{\Lambda} = \epsilon \begin{pmatrix} a & 0 & 0 \\ 0 & b & 0 \\ 0 & 0 & c \end{pmatrix}. \tag{6}$$

In this case and when

$$a = c = \frac{1}{b} \tag{7}$$

all the incident power is absorbed if the interface is flat [3].

A. Dispersion Relation and Fields in the Anisotropic Side

The electromagnetic fields in the anisotropic medium verify

$$H_x = -\frac{i}{\omega\mu_0\mu}\frac{1}{a}\frac{\partial E_z}{\partial y} \tag{8}$$

$$H_y = \frac{i}{\omega\mu_0\mu} a \frac{\partial E_z}{\partial x} \tag{9}$$

for TE polarization and

$$E_x = \frac{i}{\omega\epsilon_0\epsilon}\frac{1}{a}\frac{\partial H_z}{\partial y} \tag{10}$$

$$E_y = -\frac{i}{\omega\epsilon_0\epsilon} a \frac{\partial H_z}{\partial x} \tag{11}$$

for TM polarization. It follows that both polarization modes are ruled by the same differential equation

$$\frac{\partial^2 U}{\partial x^2} + \frac{1}{a^2}\frac{\partial^2 U}{\partial y^2} + \frac{\omega^2}{c^2}\mu\epsilon U = 0 \tag{12}$$

where $U = E_z$ for TE modes or $U = H_z$ for TM modes. It can be seen that plane-wave solutions of this equation in the form

$$U(x, y) = U_0 e^{i(k_x x + k_y y)} \tag{13}$$

verify the following dispersion relation:

$$k_x^2 + \frac{1}{a^2}k_y^2 = \frac{\omega^2}{c^2}\mu\epsilon. \tag{14}$$

B. Incident Waves

The grating is illuminated from the isotropic side by a plane wave with its incident wave vector $\vec{k}_1^i$ contained in the x–y-plane and forming an angle θ with the y-axis

$$\vec{k}_1^i = \alpha\hat{x} - \beta\hat{y} \tag{15}$$

with

$$\alpha = \frac{\omega}{c}\sqrt{\epsilon\mu}\sin(\theta) \tag{16}$$

$$\beta = \sqrt{\frac{\omega^2}{c^2}\epsilon\mu - \alpha^2}. \tag{17}$$

This wave is arbitrarily polarized and can be decomposed into a linear combination of TE and TM modes. These polarization modes can be solved separately since, due to the high symmetry of tensors $\tilde{\epsilon}$ and $\tilde{\mu}$, the boundary conditions do not couple TE and TM modes.

C. Incident and Diffracted Fields

1) Isotropic Side: The total fields $\vec{E}_1$ and $\vec{H}_1$ in the region above the grating grooves ($y > \max g(x)$) can be written as a superposition of plane waves. These plane waves may be decomposed into TE and TM modes and the z component of the fields can be expressed, for both modes, by the following same expression:

$$U_1(x, y) = U_1^i \exp\left(i\vec{k}_1^i \cdot \vec{r}\right) + \sum_{n=-\infty}^{+\infty} U_{1\,n} \exp\left(i\vec{k}_{1n} \cdot \vec{r}\right) \tag{18}$$

where

$$U_1(x, y) = \begin{cases} \vec{E}_1 \cdot \hat{z}, & \text{for the TE mode} \\ \vec{H}_1 \cdot \hat{z}, & \text{for the TM mode} \end{cases} \tag{19}$$

U_1^i is the z incident amplitude, $U_{1\,n}$ are the unknown complex amplitudes of the fields diffracted into the isotropic medium, and $\vec{k}_{1n} = \alpha_n\hat{x} + \beta_n\hat{y}$ are the diffracted wave vectors with

$$\alpha_n = \alpha + \frac{2\pi n}{d} \tag{20}$$

$$\beta_n = \sqrt{\frac{\omega^2}{c^2}\epsilon\mu - \alpha_n^2}. \tag{21}$$

The x and y components of the electric and magnetic fields are then derived through Maxwell equations.

2) Absorbing Anisotropic Side: The electromagnetic fields $\vec{E}_2$ and $\vec{H}_2$ in the region below the grating grooves ($y < \min g(x)$) are also represented by plane-wave expansions in terms of TE and TM modes. The z component of the fields for each mode can be written as follows:

$$U_2(x, y) = \sum_{n=-\infty}^{+\infty} U_{2\,n} \exp\left(i\vec{k}_{2n} \cdot \vec{r}\right) \tag{22}$$

where

$$U_2(x, y) = \begin{cases} \vec{E}_2 \cdot \hat{z}, & \text{for the TE mode} \\ \vec{H}_2 \cdot \hat{z}, & \text{for the TM mode} \end{cases} \tag{23}$$

$U_{2\,n}$ are the unknown complex amplitudes of the fields diffracted into the absorbing anisotropic medium and

$$\vec{k}_{2n} = \alpha_n\hat{x} + \gamma_n\hat{y}. \tag{24}$$

According to the dispersion relation (14)

$$\gamma_n = -\sqrt{a^2\left(\frac{\omega^2}{c^2}\epsilon\mu - \alpha_n^2\right)}. \tag{25}$$

The square root in (25) is selected in such a way that $\mathrm{Im}(\gamma_n) < 0$ (if γ_n is complex) or that $\gamma_n < 0$ (if it is real).

The x and y components of the electric and magnetic fields are then derived from (8) and (9) (for the TE mode) or (10) and (11) (for the TM mode).

D. Boundary Conditions

The boundary conditions require the continuity of the tangential components of $\vec{E}$ and $\vec{H}$ at $y = g(x)$

$$\hat{n} \times \vec{E}_1\big(x, g(x)\big) = \hat{n} \times \vec{E}_2\big(x, g(x)\big) \tag{26}$$

$$\hat{n} \times \vec{H}_1\big(x, g(x)\big) = \hat{n} \times \vec{H}_2\big(x, g(x)\big) \tag{27}$$

where $\hat{n} = (n_x, n_y, 0)$ is a unit vector normal to the interface.

These boundary conditions do not couple for TE and TM modes. By expressing the fields in (26) and (27) in terms of their z components and their derivatives—(8)–(11) for the anisotropic absorbing medium—the following equations are obtained:

$$U_1\big(x, g(x)\big) = U_2\big(x, g(x)\big) \tag{28}$$

$$\frac{\partial U_1(x,y)}{\partial x}\Big|_{y=g(x)} n_x + \frac{\partial U_1(x,y)}{\partial y}\Big|_{y=g(x)} n_y = a\frac{\partial U_2(x,y)}{\partial x}\Big|_{y=g(x)} n_x + \frac{1}{a}\frac{\partial U_2(x,y)}{\partial y}\Big|_{y=g(x)} n_y \tag{29}$$

where U_1 and U_2 are defined for each mode by (19) and (23). Thus, it can be noted that the boundary conditions take the same expressions for both modes; besides, U_1 verifies the Helmholtz equation and U_2 is ruled by (12), which are independent of the polarization. Therefore, the results will be the same for TE or TM modes.

E. Rayleigh Method

At this stage, we invoke the Rayleigh hypothesis, i.e., we assume that expansions (18) and (22), strictly valid outside the grooves, can be replaced into the boundary conditions (28) and (29). This assumption is known to give good results for gratings with shallow grooves. It holds exactly for perfectly conducting sinusoidal gratings with groove height-to-period ratios less than 0.144. However, good results have also been obtained for deeper gratings even when anisotropic materials are involved [13], [14]. To calculate the amplitudes of the diffracted fields U_{1n} and U_{2n} in terms of the amplitudes of the incident fields, we project the boundary conditions into the Rayleigh basis $\exp(i\alpha_m x)_{m=-\infty}^{+\infty}$, thus obtaining a system of linear equations, with the amplitudes U_{1n} and U_{2n} as unknowns.

The method described above has been implemented numerically. Our code is, in principle, able to deal with any single valued function $g(x)$ for the grating profile, but previous studies about the Rayleigh hypothesis [15] show that its limit of validity is highly dependent on the shape of the corrugation. For the examples shown below, we have selected sinusoidal gratings with $g(x) = (h/2)\sin(2\pi x/d)$. This kind of profile was chosen not only because it is frequently found in practical cases, but also because its performance in Rayleigh methods—either for isotropic or anisotropic gratings—is well documented [10]–[14], a fact that gives us confidence about the adequacy of this formalism for the situations that will be considered in Section III.

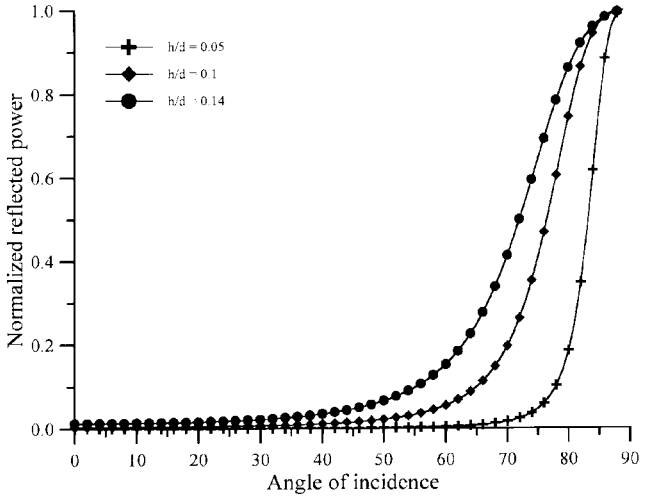

Fig. 2. Normalized reflected power as a function of the angle of incidence for $\lambda/d = 2$ and several values of h/d. Incidence is from vacuum into an anisotropic absorbing medium with $a = 1 + 3i$.

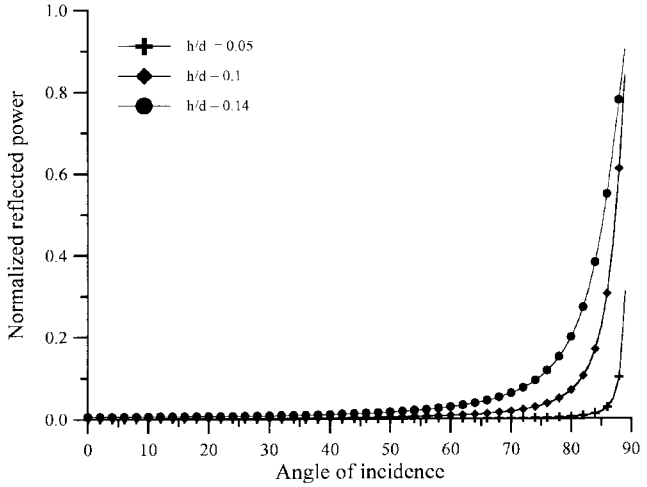

Fig. 3. Normalized reflected power as a function of the angle of incidence for $\lambda/d = 3$ and several values of h/d. Incidence is from vacuum into an anisotropic absorbing medium with $a = 1 + 3i$.

III. Results

In order to analyze how a shallow corrugation affects the reflectionless and totally absorbing characteristics of a vacuum–PML interface, we have used the theory sketched above for the case of sinusoidal gratings.

In Figs. 2 and 3, we plot the power reflected by the surface—either for TE or TM polarization, as it was explained above—as a function of the angle of incidence when the height-to-period ratio (h/d) is varied in the range $0 < h/d < 0.14$. We restrict our study to the nondiffractive-regime wavelength-to-period ratio $\lambda/d \geq 2$, where only the specularly reflected wave can be propagated. Fig. 2 shows the results for $\lambda/d = 2$ and Fig. 3 shows the results for $\lambda/d = 3$. It can be seen that, for angles of incidences $\theta < 40°$ (for $\lambda/d = 2$) or $\theta < 60°$ (for $\lambda/d = 3$), the weakly corrugated surface absorbs most of the incident power, thus behaving

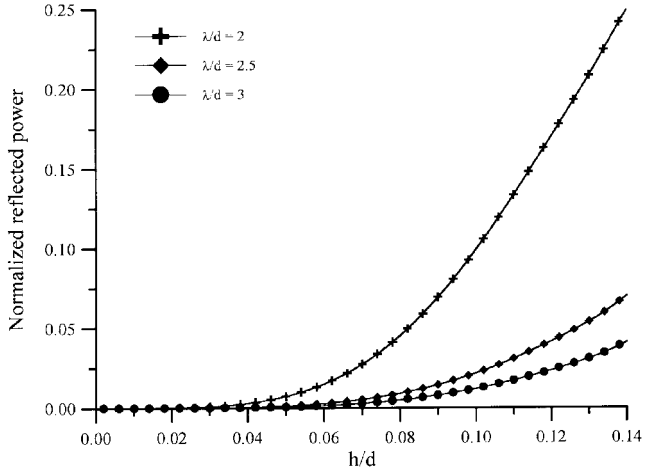

Fig. 4. Normalized reflected power as a function of h/d for $\theta = 65°$ and several values of λ/d. Incidence is from vacuum into an anisotropic absorbing medium with $a = 1 + 3i$.

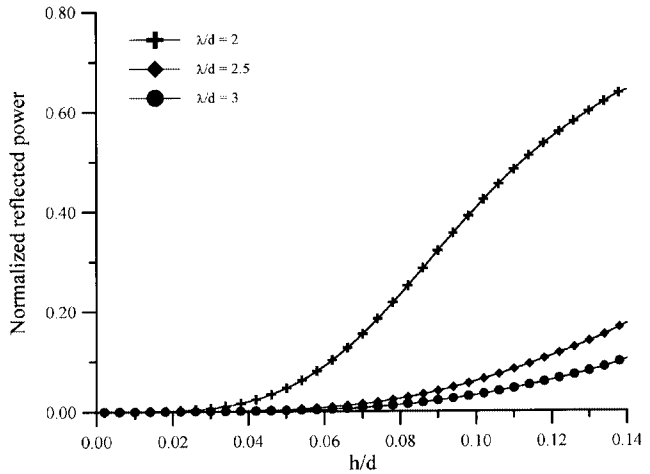

Fig. 5. Normalized reflected power as a function of h/d for $\theta = 75°$ and several values of λ/d. Incidence is from vacuum into an anisotropic absorbing medium with $a = 1 + 3i$.

practically like a PML. For example, the reflectivity of the anisotropic absorber at normal incidence is lower than 0.4% for $h/d = 0.1$.

On the other hand, for greater values of θ, the reflected power increases considerably. For example, Fig. 2 shows that over 40% of the incident power is reflected for $h/d = 0.14$ and $\theta = 70°$. In Fig. 3, for the same angle of incidence, less than 10% of the incident power is reflected, while it exceeds 20% for $\theta = 80°$. By comparing Figs. 2 and 3 for a fixed angle of incidence and for the same value of h/d, we observe that the reflectivity of the surface decreases with the wavelength. For example, for $\theta = 70°$ and $h/d = 0.14$, the reflectivity is less than 10% of the incident power for $\lambda/d = 3$ (Fig. 3), whereas for $\lambda/d = 2$ (Fig. 2), it increases four times.

In order to better analyze the influence of corrugation height on reflectivity, we have plotted the reflected power as a function of h/d in the range $0 < h/d < 0.14$ for several wavelengths and for two values of the angle of incidence: $\theta = 65°$ (Fig. 4) and $\theta = 75°$ (Fig. 5). These values were chosen in the near grazing incidence region, where the reflected power differs significantly from that of the flat surface.

From these figures, we observe that the reflectivity increases with h/d, although for very shallow corrugations ($h/d < 0.02$), the behavior of the surface remains very similar to that of a PML. In particular, Fig. 4 shows that, for $\theta = 65°$, the reflected power never exceeds 25% of the incident power for the wavelengths considered here, whereas Fig. 5 shows that the reflected power can increase to approximately 60% of the incident power for $\lambda/d = 2$ and for corrugation heights $h/d > 0.12$. This latter situation considerably differs from that of a PML. We also appreciate that higher values of λ/d correspond to lower values of the reflected power, a fact already observed in Figs. 2 and 3.

Although not shown in these figures, our numerical results confirm that for $h/d = 0$, the reflected power is zero, with an error lower than 10^{-15}.

IV. Conclusions

We have studied the effects of a periodic corrugation on the reflectivity of a flat boundary between free space and a PML anisotropic material. Using a Rayleigh method, we have observed that, for a corrugation height-to-period ratio $h/d < 0.14$ and for angles of incidence lower than 40°, the corrugated surface can still be considered a very good reflectionless absorber, although this is not the case for higher values of the angle of incidence, where nearly all the incident power may be reflected. In particular, our results show that the reflectivity of the anisotropic absorber near normal incidence remains lower than 0.4% for a 10% modulation. These results indicate that the PML concept, originally developed for planar interfaces, can be extended straightforwardly (without changing the constitutive relations of the anisotropic absorber) to weakly corrugated surfaces in problems involving fields with spatial harmonics concentrated around the region corresponding to normal incidence.

References

[1] J. P. Berenger, "A perfectly matched layer for the absorption of electromagnetic waves," *J. Comput. Phys.*, vol. 114, pp. 185–200, 1994.

[2] ——, "Three-dimensional perfectly matched layer for the absorption of electromagnetic waves," *J. Comput. Phys.*, vol. 127, pp. 363–379, 1996.

[3] Z. S. Sacks, D. M. Kingsland, R. Lee, and J. F. Lee, "A perfectly matched anisotropic absorber for use as an absorbing boundary condition," *IEEE Trans. Antennas Propagat*, vol. 43, pp. 1460–1463, Dec. 1995.

[4] W. C. Chew, J. M. Jin, and E. Michielssen, "Complex coordinate stretching as a generalized absorbing boundary condition," *Microwave Opt. Technol. Lett.*, vol. 15, no. 6, pp. 363–369, 1997.

[5] F. L. Teixeira and W. C. Chew, "PML-FDTD in cylindrical and spherical grids," *IEEE Microwave Guided Wave Lett.*, vol. 7, pp. 285–287, Sept. 1997.

[6] ——, "Systematic derivation of anisotropic PML absorbing media in cylindrical and spherical coordinates," *IEEE Microwave Guided Wave Lett.*, vol. 7, pp. 371–373, Nov. 1997.

[7] ——, "Analytical derivation of a conformal perfectly matched absorber for electromagnetic waves," *Microwave Opt. Technol. Lett.*, vol. 17, no. 4, pp. 231–236, 1998.

[8] F. L. Teixeira, K.-P. Hwang, W. C. Chew, and J.-M. Jin, "Conformal PML-FDTD schemes for electromagnetic field simulations: A dynamics stability study," *IEEE Trans. Antennas Propagat*, vol. 49, pp. 902–907, June 2001.

[9] R. Petit, *Electromagnetic Theory of Gratings*, R. Petit, Ed. Heidelberg, Germany: Springer, 1980.

[10] ——, "Plane wave expansions used to describe the field diffracted by a grating," *J. Opt. Soc. Amer.*, vol. 71, pp. 593–598, 1981.

[11] A. Wirgin, "Plane-wave expansions used to describe the field diffracted by a grating: Comments," *J. Opt. Soc. Amer.*, vol. 72, pp. 812–814, 1982.
[12] A. Lakhtakia, R. Depine, M. Inchaussandague, and V. Brudny, "Scattering by a periodically corrugated interface between free space and a gyroelectromagnetic uniaxial medium," *Appl. Opt.*, vol. 32, pp. 2765–2772, 1993.
[13] R. A. Depine and M. L. Gigli, "Diffraction from corrugated gratings made with uniaxial crystals: Rayleigh methods," *J. Mod. Opt.*, vol. 41, pp. 695–715, 1994.
[14] ——, "Conversion between polarization states at the sinusoidal boundary of a uniaxial crystal," *Phys. Rev. B, Condens. Matter*, vol. 49, pp. 8437–8445, 1994.
[15] J. A. De Santo, "Scattering from a perfectly reflecting arbitrary periodic surface: An exact theory," *Radio Sci.*, vol. 16, no. 6, p. 1315, 1981.

Marina E. Inchaussandague was born in Buenos Aires, Argentina. She received the Licenciatura degree and Ph.D. degree in physics from the Universidad de Buenos Aires (UBA), Buenos Aires, Argentina, in 1992 and 1996, respectively.

Since 1998, she is a Consejo Nacional de Investigaciones Científicas y Técnicas (CONICET) Researcher with the Departamento de Física, Facultad de Ciencias Exactas y Naturales (FCEyN), UBA.

Miriam L. Gigli was born in Lanús, Buenos Aires, Argentina. She received the Licenciatura degree and Ph.D. degree in physics from the Universidad de Buenos Aires (UBA), Buenos Aires, Argentina, in 1991 and 1996, respectively.

Since 1998, she has been a Consejo Nacional de Investigaciones Científicas y Técnicas (CONICET) Researcher and Teaching Assistant with the Departamento de Física, Facultad de Ciencias Exactas y Naturales (FCEyN), UBA.

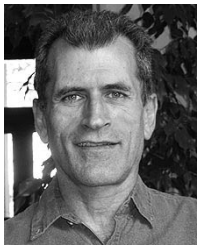

Ricardo A. Depine was born in Buenos Aires, Argentina. He received the Licenciatura degrees in physics and scientific computing and the Ph.D. degree in physics from the Universidad de Buenos Aires (UBA), Buenos Aires, Argentina, in 1976, 1978, and 1983, respectively.

He is currently a Professor with the Departamento de Física, Facultad de Ciencias Exactas y Naturales (FCEyN), UBA, where he teaches electromagnetic theory and optics, and a Consejo Nacional de Investigaciones Científicas y Técnicas (CONICET) Researcher.